

BEHAVIOUR OF FREE AND FIXED-HEAD OFFSHORE PILES UNDER CYCLIC LATERAL LOADS

*H. Ercan TAŞAN**

Received: 14.06.2016; revised: 22.03.2017; accepted: 28.04.2017

Abstract: Offshore piles are subjected to cyclic lateral loads due to environmental loads, such as wind and waves. These loads can lead to an accumulation of permanent soil deformations and excess pore water pressures in saturated soils. Finite element analyses are performed to investigate the behaviour of cyclic laterally loaded free-head and fixed piles embedded in sandy saturated soil while considering such accumulation effects. A three-dimensional fully coupled two-phase finite element is developed and implemented on the basis of a two-phase model to consider the pore water pressure development in saturated soil. In addition, a hypoplastic constitutive model is used to describe the material behaviour of sandy soil under cyclic loading. In the numerical analyses, special attention is dedicated to interactions between the pile, the saturated soil and the pore water. The results have shown that the pile displacements caused by cyclic lateral loads are significantly underestimated for both pile head conditions by approaches which do not take into account the impact of the pore water pressure development in saturated sandy soil of the pile response.

Keywords: Offshore piles, cyclic lateral loading, finite element method, fixed-head pile, free-head pile, sandy soil, accumulation, permanent displacement, pore water pressure, two-phase model

Serbest ve Rijit Başlı Açık Deniz Tekil Kazık Temellerinin Tekrarlı Yatay Yükler Etkisi Altındaki Davranışı

Öz: Açık deniz tekil kazık temelleri rüzgar ve dalga kaynaklı ağır tekrarlı yatay yüklere maruz kalmaktadır. Bu yükler nedeniyle kalıcı zemin deplasmanları ve suya doymun zeminde aşırı boşluk suyu basıncı birikimi gerçekleşebilmektedir. Çalışmada serbest ve rijit başlı tekil kazık temellerinin tekrarlı yatay yükler altındaki davranışı sonlu elemanlar yöntemi ile zeminde aşırı boşluk suyu basıncı gelişimi ve deplasman birikimi dikkate alınarak incelenmiştir. Üç boyutlu sonlu elemanlar analizlerinde, zeminde aşırı boşluk suyu basıncı gelişiminin belirlenmesi amacıyla iki fazlı modele dayanan üç boyutlu elemanlar geliştirilmiştir. Böylelikle kazığın çevresindeki zeminde boşluk suyu basıncı gelişiminin elde edilmesi mümkün olmuştur. Kumlu zemin, tekrarlı yükler altındaki davranışının modellenmesine uygun olan bir hipoplastik malzeme modeli ile tanımlanmıştır. Nümerik analizlerde özellikle kazık, suya doymun zemin ve boşluk suyu basıncı etkileşimi üzerine odaklanmıştır. Analiz sonuçları, tekrarlı yatay yük etkisindeki serbest ve rijit başlı kazıkların deplasmanlarının tahmininde, suya doymun zeminde aşırı boşluk suyu basıncı gelişimini dikkate almayan mevcut modellerin yetersiz kaldığı göstermiştir.

Anahtar Kelimeler: Tekil kazık, açık deniz, tekrarlı yatay yükleme, sonlu elemanlar yöntemi, serbest başlı tekil kazık, rijit başlı tekil kazık, kumlu zemin, kalıcı deformasyon, aşırı boşluk suyu basıncı

1. INTRODUCTION

The growing demand for energy and the increasing importance of sustainable wind energy over the past years have led to the planning of offshore wind turbines in the North Sea and in

* TRADYNA GmbH, Marie-Elisabeth-Lüders-Straße 1, 10625 Berlin-Germany
Corresponding Author: H. Ercan Taşan (tasan@tradyna.com)

the Baltic Sea. The planned constructions require special foundations due to the site and loading conditions.

Currently, common solutions which are being considered for the foundation of offshore wind turbines in the German part of the North Sea and Baltic Sea at mean sea water depths between 30 m and 40 m are the monopile, jacket and tripod foundations (Figure 1). A monopile is an open ended single steel pipe pile which is driven into predominantly saturated soil of the seabed. Driven steel tube piles as foundation elements for the jacket and tripod structures are used to transfer the loads from substructure into the soil. For this purpose, a stiff connection between pile and substructure of jacket and tripod is required which leads to a significant restriction of pile head rotation.

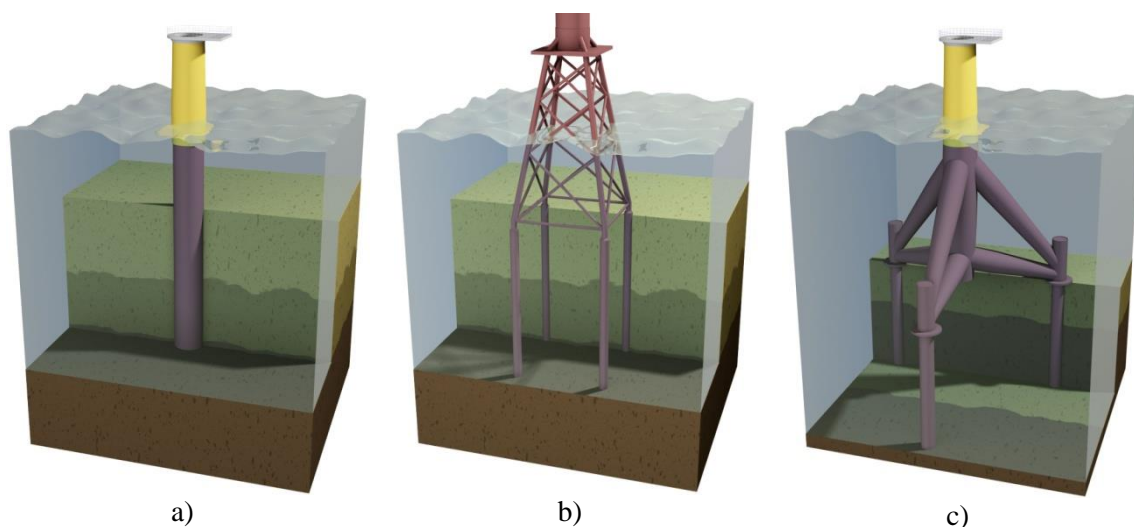


Figure 1:
Foundations for offshore wind energy turbines
a. Monopile b. Jacket c. Tripod

Apart from the usual static structure load, the foundations are subjected to continuous cyclic lateral loads caused by environmental loads, such as wind, waves and currents. The long-term cyclic loading can lead to an accumulation of permanent soil deformations as well as excess pore water pressure in saturated soil. The accumulation of excess pore water pressure is caused by the reduction of pore volume as the sand contracts under cyclic loading and the inefficiency of the soil to dissipate the excess pore water pressure completely between consecutive cycles. This results in a decrease of effective stress in the soil, which changes the stiffness of the surrounding soil and therefore the interaction of the pile and the soil (Martin et al. 1980, Cuéllar et al. 2014).

The accumulation effects in saturated soils resulting from cyclic loading can influence the ultimate strength and fatigue life of whole wind turbine structural members and should be taken into account in the design. The current design of piles subjected to cyclic lateral loading applies the p - y method according to the existing guidelines API (2014) and DNV (2014). Thereby the pile is modelled as a beam supported by a series of independent springs whose characteristics are described by nonlinear p - y curves. The p - y curves for sand are formulated on the basis of field measurements with pile diameters $d < 1,0$ m and load cycles $N \leq 100$ (Cox et al. 1974 and Reese et al. 1974). The straightforward application of these findings to piles with a large diameter and subjected to long-term cyclic lateral loading is still subject to research (Byrne et al. 2015, Carswell et al. 2015).

The p - y curves are formulated only as a function of pile diameter and do not take into account the change of pile properties such as pile bending stiffness and pile-head fixity. The

strong dependency of p - y curves on pile rigidity and pile head conditions was reported in Jamiolkowski and Garassino (1977). Furthermore, the effects of different pile parameters on p - y curves were evaluated based on the strain wedge model by Ashour and Norris (2000). The results have shown that the pile head condition is one of the significant factors for the determination of p - y curves.

New design approaches for cyclic lateral loaded piles are derived from the modification and enhancement of the models used to analyse the behaviour of piles subjected to a static load (Achmus et al. 2009, Dührkop 2009, Heidari et al. 2014). A practical design approach for the prediction of pile displacements due to irregular cyclic lateral loads which can be calibrated by means of static and cyclic triaxial test results is presented in Taşan (2012). In these design approaches, the influence of a pore water pressure development in saturated soil on the pile behaviour is not considered. However, investigations on offshore piles under cyclic lateral loads have shown that the pile response is significantly affected by pore water pressure development in soil adjacent to the piles (Cuéllar 2011, Rackwitz et al. 2012).

Three-dimensional finite element simulations are performed to investigate the behaviour of free-head and fixed-head piles subjected to cyclic lateral loading. The main focus of the numerical investigations is given on the quantitative determination of the accumulation effects in saturated soil and their impact on pile response. For this purpose, a three-dimensional fully coupled two-phase finite element is developed and implemented on the basis of the two-phase model.

2. TWO-PHASE MODEL FOR SOIL

Two-phase models are used for investigations of geotechnical problems in which the mechanical behaviour of soil is affected significantly by pore fluid. The used two-phase model has been described in detail in Zienkiewicz and Shiomi (1984) and Potts and Zdravković (1999). The principal equations of the model will be recalled in the following.

A two-phase mixture is assumed to consist of a solid phase, the skeleton, and a fluid phase which fully occupies the pores in the skeleton (Figure 2). It is assumed that the solid and fluid constituents can be modelled as incompressible.

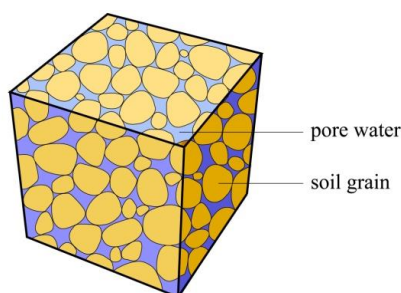


Figure 2:
Two-phase model for soil

The problem is formulated in terms of the absolute displacement of the soil skeleton \mathbf{u} and the pore water pressure p and therefore it is also known as u - p model. The balance of momentum for the mixture can be written neglecting the accelerations of the relative movement between water and skeleton and considering Terzaghi's effective stress principle by:

$$\mathbf{L}^T (\boldsymbol{\sigma}' - \mathbf{m}p) + \rho \mathbf{b} = \rho \ddot{\mathbf{u}} + \zeta \dot{\mathbf{u}} \quad (1)$$

Here, \mathbf{L} is the divergence operator, which is formulated in the following form of matrix:

$$\mathbf{L}^T = \begin{bmatrix} \partial/\partial x & 0 & 0 & \partial/\partial y & 0 & \partial/\partial z \\ 0 & \partial/\partial y & 0 & \partial/\partial x & \partial/\partial z & 0 \\ 0 & 0 & \partial/\partial z & 0 & \partial/\partial y & \partial/\partial x \end{bmatrix} \quad (2)$$

and $\boldsymbol{\sigma}'$ = effective stress vector; ρ = density of the mixture; \mathbf{b} = body forces; ζ = damping ratio and $\mathbf{m}^T = (1,1,1,0,0,0)$.

The mass balance of fluid phase is formulated as

$$\mathbf{m}^T \mathbf{L} \dot{\mathbf{u}} - \nabla^T \frac{\mathbf{k}_p}{\eta_w} \nabla p + \nabla^T \frac{\mathbf{k}_p}{\eta_w} \rho_w \mathbf{b} = 0 \quad (3)$$

with \mathbf{k}_p = permeability matrix, ρ_w = the density of water and η_w = the dynamic viscosity of water.

For isotropic problems the permeability matrix can be written as $\mathbf{k}_p = k_p \mathbf{I}$ with unit matrix \mathbf{I} . The hydraulic conductivity k_d can be derived from the permeability k_p by

$$k_d = \frac{\rho_w g}{\eta_w} k_p, \quad (4)$$

where g is the gravity acceleration. A domain Ω with boundary Γ is filled with the mixture. The boundary conditions to be prescribed for Equation (1) and (3) are displacements $\bar{\mathbf{u}}$ on solid displacement boundary Γ_u , surface tractions $\bar{\boldsymbol{\sigma}}$ on solid traction Γ_t boundary, pore water pressure \bar{p} on fluid pressure boundary Γ_p and surface flow \bar{q} on fluid flux boundary Γ_q .

The Equations (1) and (3) are discretized using standard Galerkin techniques. Thereby the displacement and pore water pressure fields are approximated as

$$\mathbf{u} = \mathbf{N}_u \bar{\mathbf{u}}, \quad p = \mathbf{N}_p \bar{\mathbf{p}}, \quad (5)$$

where \mathbf{N}_u and \mathbf{N}_p are the shape functions, $\bar{\mathbf{u}}$ and $\bar{\mathbf{p}}$ are corresponding vectors of unknowns. The following matrix equations are finally determined:

$$\mathbf{M} \ddot{\bar{\mathbf{u}}} + \mathbf{C} \dot{\bar{\mathbf{u}}} + \mathbf{K} \bar{\mathbf{u}} - \mathbf{Q} \bar{\mathbf{p}} = \mathbf{f}_u, \quad (6)$$

$$\mathbf{Q}^T \dot{\bar{\mathbf{u}}} + \mathbf{H} \bar{\mathbf{p}} = \mathbf{f}_p, \quad (7)$$

with the mass matrix $\mathbf{M} = \int_{\Omega} \mathbf{N}_u^T \rho \mathbf{N}_u d\Omega$, the damping matrix $\mathbf{C} = \int_{\Omega} \mathbf{N}_u^T \zeta \mathbf{N}_u d\Omega$, the structural stiffness matrix $\mathbf{K} = \int_{\Omega} \mathbf{B}^T \mathbf{D}_T \mathbf{B} d\Omega$, the coupling matrix $\mathbf{Q} = \int_{\Omega} \mathbf{B}^T \mathbf{m} \mathbf{N}_p d\Omega$, the load vector of solid $\mathbf{f}_u = \int_{\Omega} \mathbf{N}_u^T \rho \mathbf{b} d\Omega + \int_{\Gamma} \mathbf{N}_u^T \bar{\boldsymbol{\sigma}} d\Gamma$, the permeability matrix $\mathbf{H} = \int_{\Omega} \mathbf{B}_p^T \mathbf{k}_p \mathbf{B}_p d\Omega$ and the load vector of fluid $\mathbf{f}_p = \int_{\Omega} \mathbf{B}_p^T \mathbf{k}_p \rho_w \mathbf{b} d\Omega - \int_{\Gamma} \mathbf{N}_p^T \bar{q} d\Gamma$.

$\mathbf{B} = \mathbf{L} \mathbf{N}_u$ and $\mathbf{B}_p = \nabla \mathbf{N}_p$ are the matrices of the derivatives of shape functions. \mathbf{D}_T is the matrix of tangential moduli, which may be determined from a nonlinear stress-strain relationship.

Generalized Newmark method, which is described in Bathe (1996), is used for time integration of the coupled equations (6) and (7).

The described $u-p$ model is valid for most geotechnical problems associated with water-saturated sandy soils unless high-frequency oscillations occur (Zienkiewicz et al. 1980).

3. 3D TWO-PHASE ELEMENT

As shown in Figure 3, a 3D continuum element u20p8 on the basis of the two-phase model is implemented, where the displacement field is approximated using triquadratic interpolation functions, and the pressure field is approximated using trilinear interpolation functions.

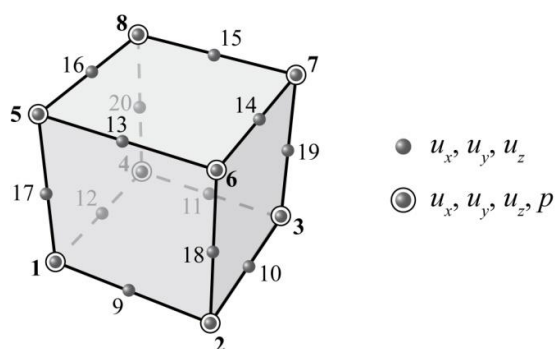


Figure 3:
3D two-phase element

A well-known problem with modelling two-phase elements is the numerical instability, which can be observed in the form of pore water pressure oscillations (Mased and Hughes 2002, Pastor et al. 1997). A high order interpolation of the displacement field is required to overcome unstable tendencies of the finite elements (Zienkiewicz 1986).

The numerical examples to verify the two-phase model and the implemented u20p8 element are presented in Taşan et al. (2010).

4. HYPOPLASTIC CONSTITUTIVE LAW

Cohesionless soils can be modelled by hypoplastic constitutive law considering the influence of stress level and soil density on the soil behaviour. Stiffness, dilatancy, contractancy and peak friction is followed by the soil state and the deformation direction. Plastic deformations are simulated without using potential or switch functions. A single tensorial equation is used to describe plastic as well as elastic deformations.

The basic hypoplastic theory (Kolymbas 1988, Bauer 1996, von Wolfersdorf 1996, Herle 1997) is expanded by Niemunis and Herle (1997) to model realistically the accumulation effects and the hysteretic material behaviour under cyclic loading. An additional state variable, which is the intergranular strain, is introduced to consider the influence of changing direction of deformation on the mechanical behaviour of soil.

A total of eight material parameters are required for the basic hypoplastic model. The description and experimental determination of the material parameters are explained in detail in Herle (1997). The expanded model with intergranular strain requires five additional parameters (Niemunis and Herle 1997).

The suitability of the material model using the u20p8 element was confirmed in Taşan et al. (2010).

5. FINITE ELEMENT MODEL

A three-dimensional finite element model was developed to investigate the behaviour of offshore piles under cyclic lateral loading, taking the interaction between the pile and the surrounding sandy subsoil into account. A single free- and fixed-head pile with an embedded length $l = 36.0$ m, an external diameter $d = 2.6$ m and wall thickness $t_d = 0.06$ m is modelled (Figure 4).

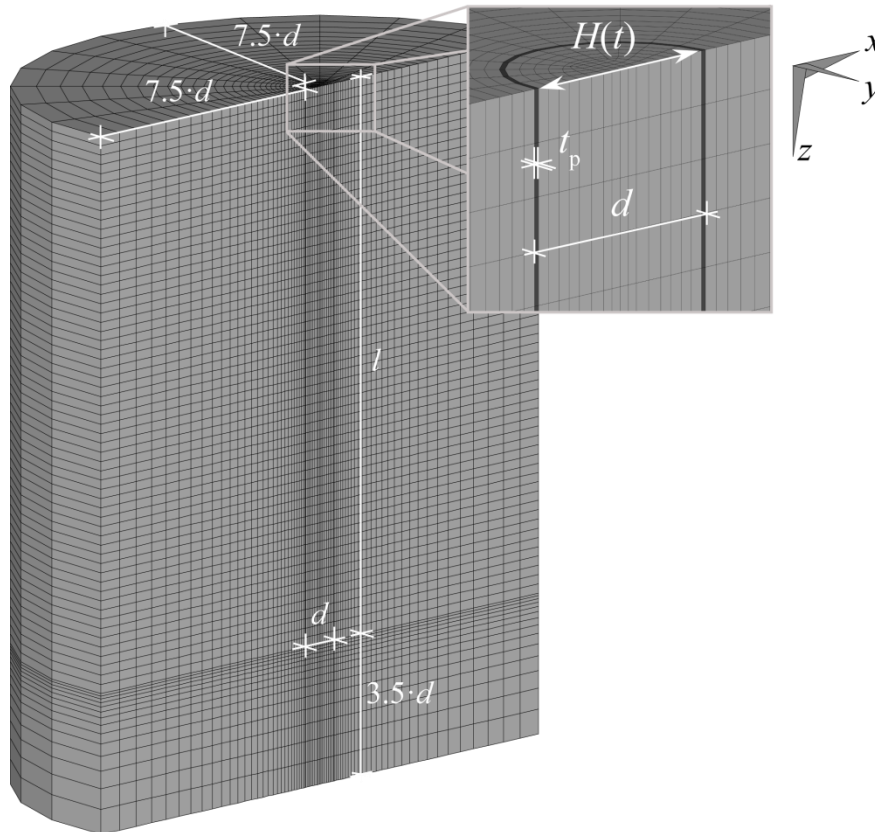


Figure 4:
FE mesh of soil-pile system

With regard to the symmetry of both geometrical and loading conditions, only one half of the soil-pile system is considered in order to reduce computational effort. The mesh fineness and model dimensions, which are given in Figure 4, are sufficient to obtain sufficiently accurate results and avoid an impact of the boundary conditions.

The boundary conditions, which imposed on mesh, are fixing of nodes at the bottom of the mesh against displacement in all directions, on the plane of symmetry against displacement normally on that plane and on the periphery of the mesh against displacement in both horizontal directions. Furthermore, non-permeable conditions are assumed on all boundaries, except boundaries on model surface, where pore pressure due to existing mean sea water level must be considered. In case of free-head pile, the nodes along the pile head are free to move in all directions. For simulation of fixed-head pile conditions the nodes along the pile head are constrained so that the rotation of pile head is hindered.

The 3D two-phase u20p8 elements are used for modelling the saturated sandy soil with submerged unit weight $\gamma' = 11.3$ kN/m³, initial relative density $I = 0.92$ and hydraulic

conductivity $k_d = 2.0 \cdot 10^{-4}$ m/s representing the sandy soil conditions in situ. The hypoplastic material parameters of sand are given in Table 1.

Table 1. Hypoplastic material parameters of modelled sand

φ_c (°)	h_s (MPa)	n	e_{d0}	e_{c0}	e_{i0}	α	β
32.0	3730	0.20	0.41	0.74	0.89	0.14	1.0
	R	m_R	m_T	β_r	χ		
	$1 \cdot 10^{-4}$	5.0	2.0	0.4	6.0		

The basic hypoplastic constitutive model requires the parameters critical friction angle φ_c , the lower and upper bound void ratio of a grain skeleton at zero pressure e_{d0} and e_{i0} . A further limit void ratio model parameter is e_{c0} , which represents the void ratio in a critical state at zero pressure. The constant h_s describes a reference pressure-independent stiffness, the so called granular hardness, together with the exponent n govern the compression for an increasing effective mean pressure. The dilatancy behaviour of the sandy soil is directly related by an exponent α that controls the peak friction angle. The constant β is an exponent in the hypoplastic model which influences the stress rate with increasing soil density at constant strain rate. The description and experimental determination of the basic hypoplastic material parameters are explained in detail in Herle (1997) and Rondón et al. (2007). The expanded hypoplastic model with intergranular strain requires the additional parameters – maximum value of intergranular strain R , increase factors m_R and m_T , the exponents β_r and χ (Niemunis and Herle 1997).

A linear elastic material behaviour with Young’s modulus $E = 2.1 \cdot 10^8$ kN/m² and Poisson’s ratio $\nu = 0.3$ is assumed for the open ended tubular steel pile which is modelled with 20 node continuum elements. The frictional behaviour in the interface between pile and soil is modelled by elasto-plastic contact. For this purpose, surface contact elements with a contact friction angle of $\delta = 21^\circ$ are used.

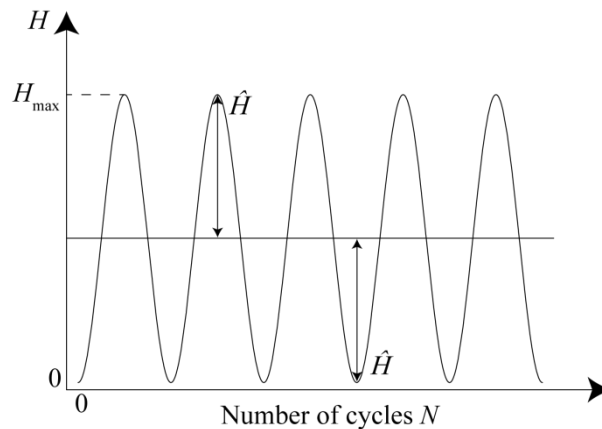


Figure 5:
Characteristic of applied cyclic lateral load

Prior to the first phase of the simulation, a vertical and a horizontal effective stress as the initial loading must be defined for soil to determine the required state variables of the expanded hypoplastic model. Therefore, as first a calculation under gravity loading is performed with a value of the coefficient of earth pressure at rest $k_0 = 0.5$. The static water pressure resulting from mean sea water level of 40.0 m is thereby also determined. In the next step the predefined soil elements defining the pile geometry are replaced by pile elements and thereby the contact

between the pile and surrounding soil is activated. Subsequently, the cyclic lateral load as shown in Figure 5 is applied on the pile head at the soil surface level.

The characteristic of cyclic lateral load is idealized on the basis of wind, wave and current loads to investigate the accumulation effects in sandy soil. Here, a cyclic lateral load with an amplitude of $\hat{H} = 400$ kN and frequency $f = 0.16$ Hz is applied on the pile head. The maximum cyclic lateral load H_{\max} in Figure 5 and the loading frequency were determined according to design load case power production of offshore wind turbine according to DNV (2014). Therefore, a pile of four-legged jacket structure planned in German part of the North Sea at mean water depth of 40 m is considered.

6. PORE WATER PRESSURE DEVELOPMENT

Contour plots of pore water pressure ratio $\Delta p/(\gamma'z)$, which is defined as a change in pore water pressure with respect to initial vertical effective stress, are shown for free-head pile in Figure 5 and for fixed-head pile in Figure 6. Both piles start to load in positive x -direction.

At the beginning of the loading, the compaction of saturated sand in the passive side lead to a reduction of the sand volume and hence to a development of excess pore water pressure in sand for both pile head conditions (Figure 5a and Figure 6a). In the case of free-head pile condition, the sandy soil close to the pile shaft up to a depth of $0.19l$ below the sea ground surface is affected due to pore water pressure development. Excess pore water pressures determined from the analysis for fixed-head pile influence the shear strength of the sand adjacent to the pile shaft especially to a depth of $0.14l$ beneath the seabed surface.

During the first loading cycle, the pore volume of sand in the active side is increased with the extension of the grain skeleton, as a consequence, negative pore water pressure is determined, which is dissipated progressively by the following load cycles (Figure 5a and Figure 6a).

A dissipation of excess pore water pressures occurs in different directions. Besides the excess pore water flow towards seabed surface, dissipation takes place in radial as well as in tangential direction with regard to the pile.

With the increasing number of loading cycles, the influenced soil region is expanded and an accumulation of excess pore water is observed for a free-head pile condition (Figure 5b and Figure 5c). Thereby, the accumulated pore water pressure reaches the range of the initial vertical soil stress directly below the seabed surface close to pile shaft. The accumulation is caused by the cyclic compression of the soil (and hence reduction of pore volume) with the result of pore water pressure build-up and the inability of the soil to dissipate the excess pore water pressure completely between consecutive cycles. For the case of fixed-head pile, the calculated pore water pressure development is nearly unchanged by further cyclic loading and an accumulation of excess pore water pressures is not observed (Figure 6b and Figure 6c).

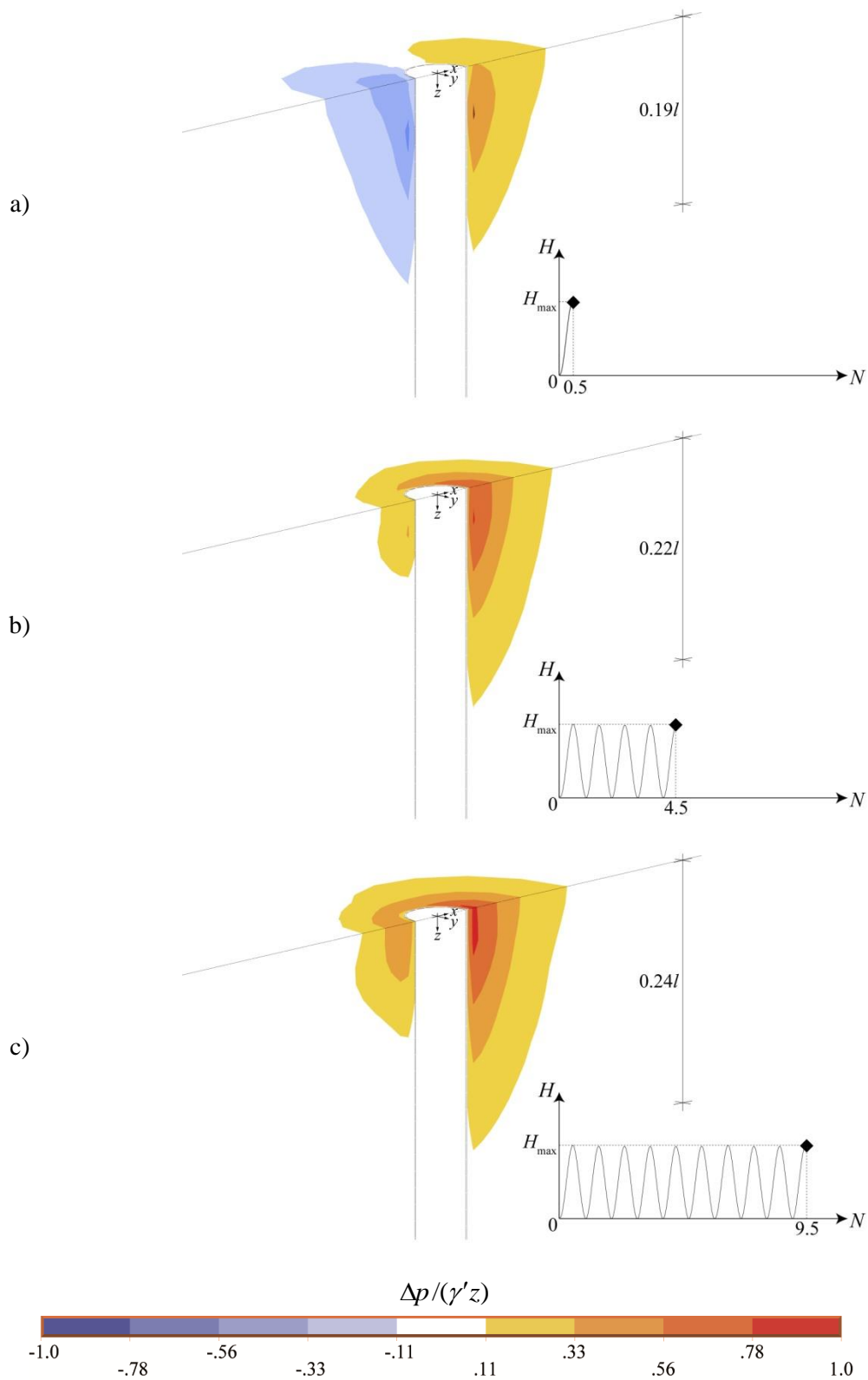


Figure 6:
 Contour plot of changes in pore water pressure with respect to initial vertical effective stresses for free-head pile;
 a. $N = 0.5$ b. $N = 4.5$ c. $N = 9.5$

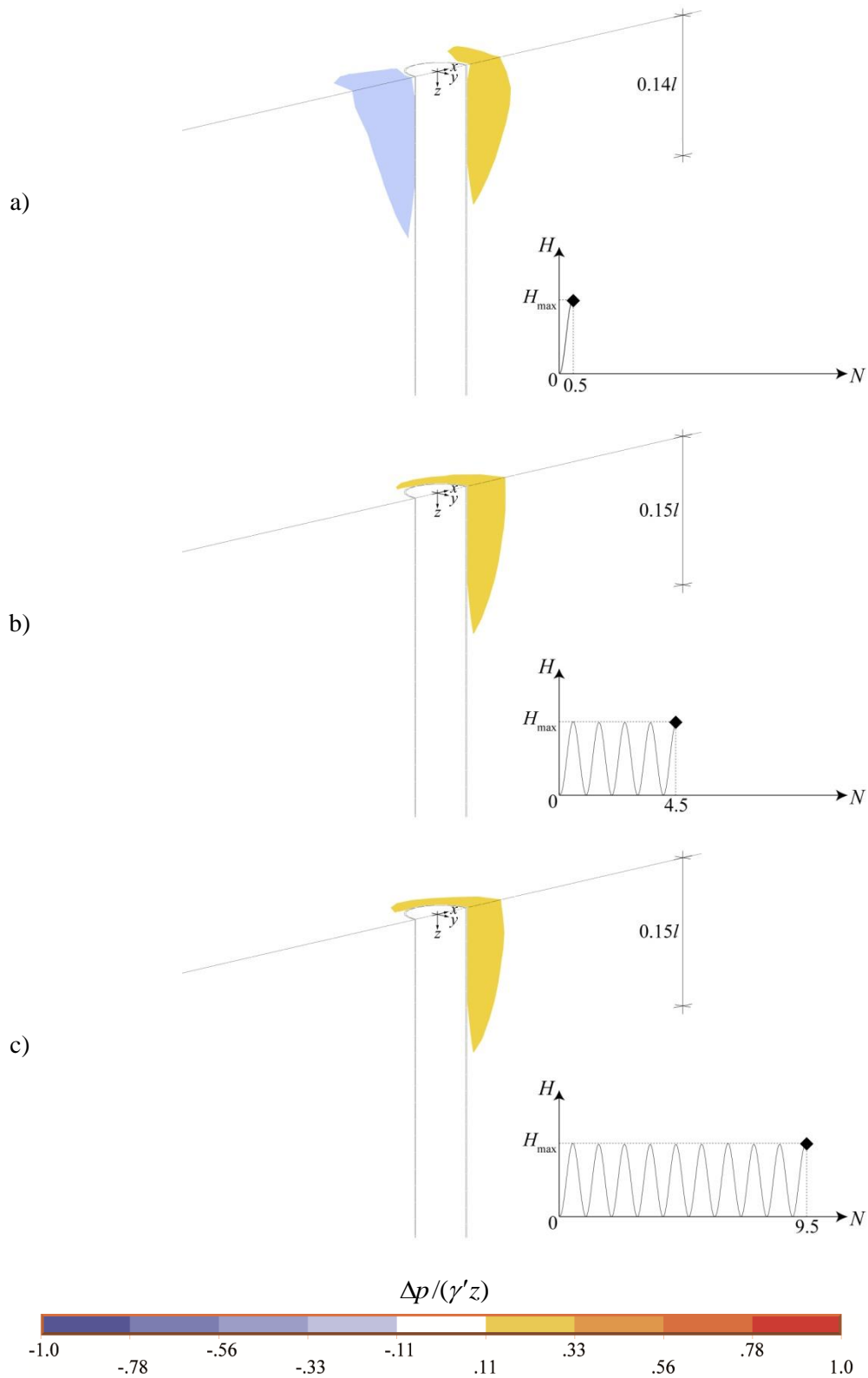


Figure 7:
 Contour plot of changes in pore water pressure with respect to initial vertical effective stresses
 for fixed-head pile;
 a. $N = 0.5$ b. $N = 4.5$ c. $N = 9.5$

7. PILE DISPLACEMENTS

The lateral displacements of pile versus depth below sea ground at loading cycles $N = 0.5, 3.5, 6.5$ and 9.5 are shown for the free-head pile in Figure 7 and for fixed-head pile in Figure 8. The pile displacements consist of reversible as well irreversible parts of displacements.

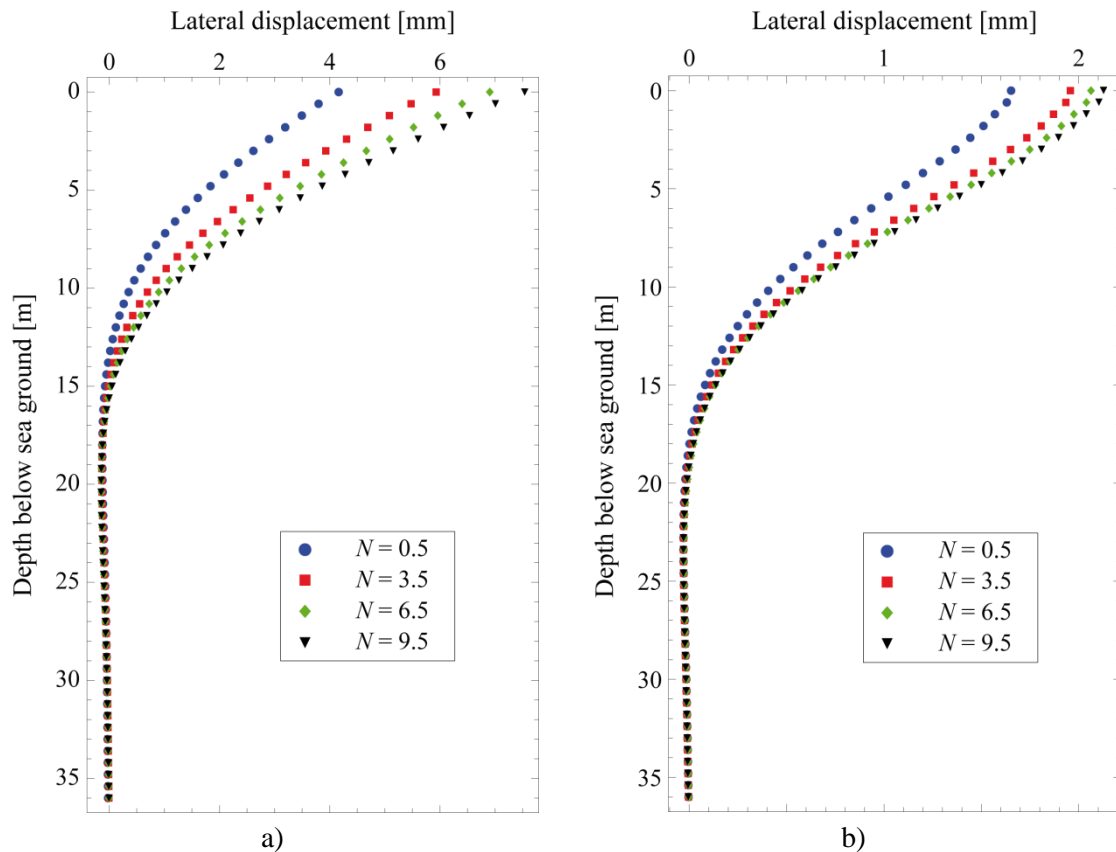


Figure 8:
Displacements of pile versus depth below sea ground at loading cycles $N=0.5, 3.5, 6.5$ and 9.5 ;
a. free-head pile b. fixed-head pile

The finite element results have shown an accumulation of pile head displacements with an increasing number of loading cycles for both pile head conditions. The increase of pile displacements at the beginning of the loading is markedly high. By further cyclic loading, the displacement changes per loading cycle are reduced, and a stabilisation of pile response is determined. In addition, a moving of first zero crossing of the pile deflection in the direction to pile base with increasing loading cycles is obtained.

The lateral pile head displacements in dependence of the number of loading cycles are depicted for free-head pile in Figure 7 and for fixed-head pile in Figure 8. For comparison, the displacements are also plotted, which is obtained by finite element calculations with using standard 20 node continuum elements combined with hypoplastic constitutive model for the modelling of soil. In this case, an influence of pore water development in saturated soil on the pile behaviour cannot be considered. In addition to the results of finite element analyses, the displacements obtained through the p - y method according to guideline API (2014) are shown in Figure 9 and Figure 10. The p - y method does not consider the impact of pore water pressure development in saturated soil of pile behaviour and the calculated displacements are not dependent on the number of loading cycles.

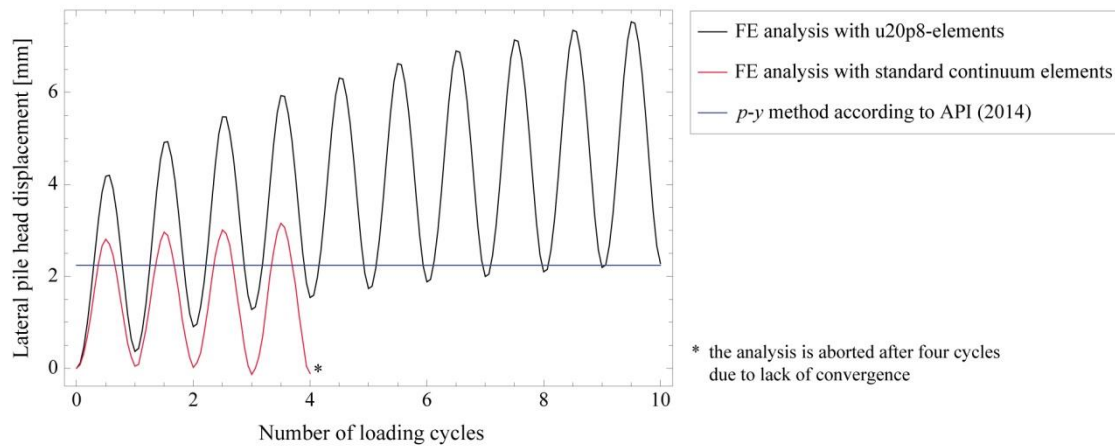


Figure 9:
Lateral pile head displacements in dependence of number of loading cycles for free-head pile condition

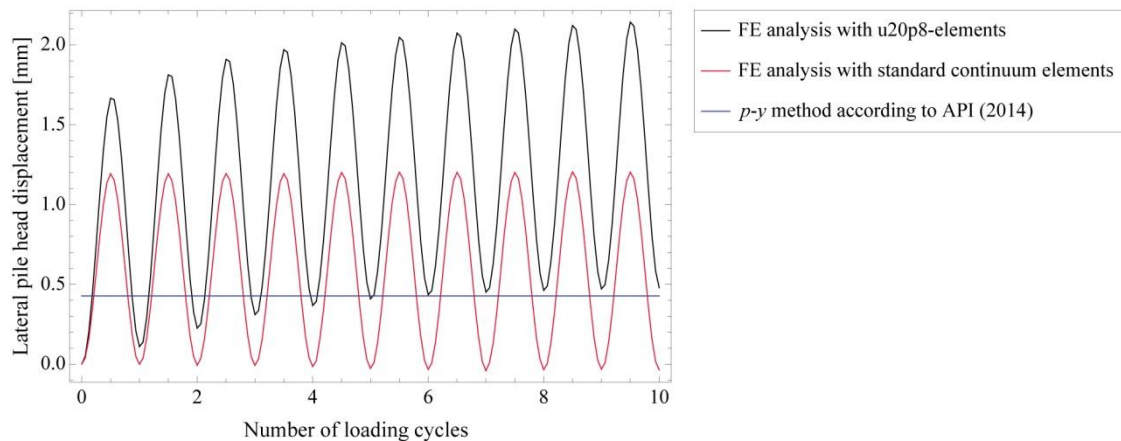


Figure 10:
Lateral pile head displacements in dependence of number of loading cycles for fixed-head pile condition

The results of finite element calculations with u20p8-elements indicate the development of reversible and irreversible pile head displacements with an increasing number of cyclic loading. An accumulation of irreversible pile head displacements with continuously decreasing rate is evident for both pile head conditions. A stabilisation of irreversible pile displacements with cyclic loading occurs. The reversible as well as irreversible displacements are significantly underestimated by other approaches which do not take into account the effect of pore water development in saturated sand.

8. CONCLUSION

The behaviour of a free-head and fixed-head offshore piles subjected to cyclic lateral load was investigated by means of the finite elements method. In the finite element analyses, a fully coupled two-phase model combined with a hypoplastic constitutive model for the water saturated soil are used for realistic determination of interactions between the pile, saturated soil and pore water. The special focus is given to the influence of cyclic loading on the pore water pressure accumulation in saturated soil and the lateral displacement accumulation of piles.

The results of finite element simulations for investigated offshore piles provide the main following conclusions:

- An accumulation of pore water pressure in saturated soil due to cyclic loading can occur and the accumulated pore water pressure can reach the range of the initial vertical soil stress in the near surface soil-pile interaction region.
- An accumulation of pile head displacements with an increasing number of loading cycles are determined for both pile head conditions. A markedly high increase of pile head displacements takes place at the beginning of the loading. By further cyclic loading, a reduction of displacement changes per loading cycle and a stabilisation of pile response are obtained.
- Pile displacements are significantly underestimated for both pile head conditions by approaches which do not take into account the impact of the pore water pressure development in saturated sandy soil of the pile response.

The aim of these investigations is to propose a practical design method for cyclic laterally loaded piles by considering the varying pile head conditions and the impact of pore water pressure development in saturated soil on the pile response. Therefore, further numerical and experimental investigations are planned.

REFERENCES

1. Achmus, M., Kuo, Y.-S. and Abdel-Rahman, K. (2009) Behavior of monopile foundations under cyclic lateral load, *Computers and Geotechnics*, 36, 725–735. DOI: doi.org/10.1016/j.compgeo.2008.12.003
2. API (2014) American Petroleum Institute, Recommended Practice 2A-WSD Planning, Designing, and Constructing Fixed Offshore Platforms - Working Stress Design.
3. Ashour, M. and Norris, G. (2000) Modeling lateral soil-pile response based on soil-pile interaction, *Journal of Geotechnical and Geoenvironmental Engineering*, 126(5), 420–428. DOI: dx.doi.org/10.1061/(ASCE)1090-0241(2000)126:5(420)
4. Bathe, K.-J. (1996) Finite element procedures, New Jersey: Prentice Hall.
5. Bauer, E. (1996) Calibration of a comprehensive hypoplastic model for granular materials, *Soils and Foundations*, 36(1), 13–26, 1996. DOI: doi.org/10.3208/sandf.36.13
6. Byrne, B.W., McAdam, R., Burd, H.J., Houlsby, G.T., Martin, C.M., Zdravković, L., Taborda, D.M.G., Potts, D.M., Jardine, R.J., Sideri, M., Schroeder, F.C., Gavin, K., Doherty, P., Igoe, D., Muir Wood, A., Kallehave, D. and Skov Gretlund, J. (2015) New design methods for large diameter piles under lateral loading for offshore wind applications, Proceedings of the Third International Symposium of Frontiers in Offshore Geotechnics (ISFOG2015), Norway.
7. Carswell, W., Fontana, C., Arwade, S.R., DeGroot, D.J. and Myers, A.T. (2015) Comparison of cyclic p-y methods for offshore wind turbine monopiles subjected to extreme storm loading, Proceedings of the ASME 2015 34th International Conference on Ocean, Offshore and Arctic Engineering (OMAE 2015), Volume 9: Ocean Renewable Energy, Canada. DOI: 10.1115/OMAE2015-41312
8. Cox, W.R., Reese, L.C. and Grubbs, B.R. (1974) Field testing of laterally loaded piles in sand, Proceedings of the Sixth Offshore Technology Conference, OTC 2079, Houston, 459–472. DOI: doi.org/10.4043/2079-MS
9. Cuéllar, P. (2011) Pile Foundations for Offshore Wind Turbines: Numerical and Experimental Investigations on the Behaviour under Short-Term and Long-Term Cyclic Loading, Doctoral Thesis, TU Berlin. DOI: dx.doi.org/10.14279/depositonce-2760

10. Cuéllar, P., Mira, P., Pastor, M., Merodo, J.A.F.M., Baeßler, M. and Rucker, W. (2014) A numerical model for the transient analysis of offshore foundations under cyclic loading, *Computers and Geotechnics*, 59(6), 75–86. DOI:10.1016/j.compgeo.2014.02.005
11. DNV (2014) Det Norske Veritas, Offshore Standard DNV–OS–J101, Design for Offshore Wind Turbine Structures.
12. Dührkop, J. (2009) Zum Einfluss von Aufweitungen und zyklischen Lasten auf das Verformungsverhalten lateral beanspruchter Pfähle in Sand, Veröffentlichungen des Institutes für Geotechnik und Baubetrieb der Technischen Universität Hamburg-Harburg, Heft 20.
13. Heidari, M., El Naggar, H., Jahanandish, M. and Ghahramani, A. (2014) Generalized cyclic p-y curve modeling for analysis of laterally loaded pile, *Soil Dynamics and Earthquake Engineering*, 63, 138–49. DOI: 10.1016/j.soildyn.2014.04.001
14. Herle, I. (1997) Hypoplastizität und Granulometrie einfacher Korngerüste, Veröffentlichung des Institutes für Bodenmechanik und Felsmechanik der Universität Fridericana in Karlsruhe, Heft 142.
15. Jamiolkowski, M. and Garassino, A. (1977), Soil modulus for laterally loaded piles, Proceedings of the 9th International Conference of Soil Mechanics and Foundation Engineering, Tokyo, 43–58.
16. Kolymbas, D. (1988) Eine konstitutive Theorie für Böden und andere körnige Stoffe, Veröffentlichung des Institutes für Bodenmechanik und Felsmechanik der Universität Fridericana in Karlsruhe, Heft 109.
17. Martin, G.R., Lam, I. and Tsai, C.-F. (1980) Pore-pressure dissipation during offshore cyclic loading, *Journal of the Geotechnical Engineering Division*, 106(9), 981–996.
18. Masud, A. and Hughes, T.J.R (2002) A stabilized mixed finite element method for Darcy flow, *Computer Methods in Applied Mechanics and Engineering*, 191, 4341–4370. DOI: doi.org/10.1016/S0045-7825(02)00371-7
19. Niemunis, A. and Herle, I. (1997) Hypoplastic model for cohesionless soils with elastic strain range, *Mechanics of Cohesion-Fractional Materials*, 2(4), 279–299. DOI: 10.1002/(SICI)1099-1484(199710)2:4<279::AID-CFM29>3.0.CO;2-8
20. Pastor, M., Li, T. and Merodo, J.A.F. (1997) Stabilized finite elements for harmonic soil dynamics problems near the undrained-incompressible limit, *Soil Dynamics and Earthquake Engineering*, 16, 161–171. DOI: doi.org/10.1016/S0267-7261(97)00046-8
21. Potts, D.M. and Zdravković, L. (1999) Finite element analysis in geotechnical engineering - theory. London: Thomas Telford.
22. Rackwitz, F., Savidis, S. and Taşan, H.E. (2012) New design approach for large diameter offshore monopiles based on physical and numerical modelling, In: Hryciw, R.D., Athanasopoulos-Zekkos, A. and Yesiller, N. (eds.): Geotechnical Special Publication GSP No. 225 Geo-Congress 2012, State of the Art and Practice in Geotechnical Engineering, Proc. GeoCongress 2012, March 25-29, Oakland, CA, ASCE, 356–365. ISBN: 978-0-7844-1212-1
23. Reese, L.C., Cox, W.R. and Koop, F.D. (1974) Analysis of Laterally Loaded Piles in Sand, Proceedings of the Sixth Offshore Technology Conference, OTC 2080, Houston, 2, 473–483. DOI: doi.org/10.4043/2080-MS.

24. Rondón, H.A., Wichtmann, T., Triantafyllidis, Th. and Lizcano, A. (2007) Hypoplastic material constants for a well-graded granular material (UGM) for base and subbase layers of flexible pavements, *Acta Geotechnica*, 1(2), 113–126. DOI: 10.1007/s11440-007-0030-3
25. Taşan, H.E., Rackwitz, F. and Savidis, S. (2010) Behaviour of cyclic laterally loaded large diameter monopiles in saturated sand, Proceedings of the 7th European Conference on Numerical Methods in Geotechnical Engineering, NUMGE, Trondheim, Norway, 889–894.
26. Taşan, H.E. (2012) Prognose der Verschiebungen von zyklisch lateral belasteten Monopiles in geschichteten Böden, *Bauingenieur*, 87(6), 297–305.
27. von Wolffersdorff, P.-A. (1996) A hypoplastic relation for granular materials with a predefined limit state surface, *Mechanics of Cohesive-Frictional Materials*, 1(3), 251–271. DOI: 10.1002/(SICI)1099-1484(199607)1:3<251::AID-CFM13>3.0.CO;2-3
28. Zienkiewicz, O.C., Chang, C.T. and Bettés, P. (1980) Drained, undrained, consolidating dynamic behaviour assumptions in soils. *Géotechnique*, 30(4), 385–395. DOI: 10.1680/geot.1980.30.4.385
29. Zienkiewicz, O.C. and Shiomi, T. (1984) Dynamic behaviour of saturated porous media; the generalized Biot formulation and its numerical solution, *International Journal of Numerical Analytical Methods in Geomechanics*, 8(1), 71–96. DOI: 10.1002/nag.1610080106
30. Zienkiewicz, O.C. (1986) The patch test for mixed formulations, *International Journal for Numerical Methods in Engineering*, 23(10), 1873–1883. DOI: 10.1002/nme.1620231007

